Photoactive Yellow Protein from the Halophilic Bacterium *Salinibacter ruber*

Samy Memmi,[‡] John Kyndt,[‡,§] Terry Meyer,[§] Bart Devreese,[‡] Michael Cusanovich,[§] and Jozef Van Beeumen*[,‡]

Laboratory of Protein Biochemistry and Protein Engineering, Ghent University, K.L. Ledeganckstraat 35, B-9000 Ghent, Belgium, and Department of Biochemistry and Molecular Biophysics, University of Arizona, Tucson, Arizona 85721

Received July 26, 2007; Revised Manuscript Received November 27, 2007

ABSTRACT: A gene for photoactive yellow protein (PYP) was identified from the genome sequence of the extremely halophilic aerobic bacterium *Salinibacter ruber* (Sr). The sequence is distantly related to the prototypic PYP from *Halorhodospira halophila* (Hh) (37% identity) and contains most of the amino acid residues identified as necessary for function. However, the Sr *pyp* gene is not flanked by its two biosynthetic genes as in other species. To determine as to whether the Sr *pyp* gene encodes a functional protein, we cloned and expressed it in *Escherichia coli*, along with the genes for chromophore biosynthesis from *Rhodobacter capsulatus*. The Sr PYP has a 31-residue N-terminal extension as compared to other PYPs that appears to be important for dimerization; however, truncation of these extra residues did not change the spectral and photokinetic properties. Sr PYP has an absorption maximum at 431 nm, which is at shorter wavelengths than the prototypical Hh PYP (at 446 nm). It is also photoactive, being reversibly bleached by either blue or white light. The kinetics of dark recovery is slower than any of the PYPs reported to date (4.27×10^{-4} s^{-1} at pH 7.5). Sr PYP appears to have a normal photocycle with the I_1 and I_2 intermediates. The presence of the I_2' intermediate is also inferred on the basis of the effects of temperature and alchohol on recovery. Sr PYP has an intermediate spectral form in equilibrium with the 431 nm form, similar to *R. capsulatus* PYP and the Y42F mutant of Hh PYP. Increasing ionic strength stabilizes the 431 nm form at the expense of the intermediate spectral form, and the kinetics of recovery is accelerated 6.4-fold between 0 and 3.5 M salt. This is observed with ions from both the chaotropic and the kosmotropic series. Ionic strength also stabilizes PYP against thermal denaturation, as the melting temperature is increased from 74 °C in buffer alone to 92 °C in 2 M KCl. Sr accumulates KCl in the cytoplasm, like *Halobacterium*, to balance osmotic pressure and has very acidic proteins. We thus believe that Sr PYP is an example of a halophilic protein that requires KCl to electrostatically screen the excess negative charge and stabilize the tertiary structure.

Organisms are subjected to a variety of environmental stimuli to which they respond and adapt. The information from light stimuli is recorded by photosensory proteins, specially adapted to absorb particular wavelengths of the solar spectrum and transmitting the signals to intracellular response regulators. They solely function in signal transduction, monitoring the environmental light quality, quantity, and direction, and have to be considered separately from the specialized photosynthetic pigments that convert solar energy to chemical energy for growth and development. Light absorption in biological signal transfer is conducted by a number of photosensory families, each characterized by the binding of a chromophore from a particular class of chemical compound: rhodopsins with retinal (*1*); phytochromes with tetrapyrrole (*2*); phototropins, cryptochrome (*3*), and BLUF-proteins with FMN (*4*); and photoactive yellow proteins (PYPs[1]) with *p*-hydroxy-cinnamic acid (*5*). The latter family currently consists of a set of 20 homologous photoreceptors from 13 bacterial species (*6*) and five isolated from unidentified bacteria in seawater samples (*7*). The prototypic photoactive yellow protein (Hh PYP), first isolated from the phototrophic bacterium *Halorhodospira* (formerly *Ectothiorhodospira*) *halophila* (*8*) has a wavelength maximum at 446 nm ($\epsilon = 45$ mM^{-1} cm^{-1}) and is a 14 kDa water-soluble, cytoplasmic blue-light photoreceptor. The PYP chromophore is covalently bound to a conserved cysteine residue via a thioester linkage. Upon blue-light illumination, PYP enters a photocycle during which the chromophore undergoes trans−cis isomerization and the 446 nm absorption maximum is bleached and blue-shifted to ∼350 nm within milliseconds and recovers in the dark within 1 s (*9*). Several intermediates of the Hh PYP photocycle have been identified based on their spectral and temporal changes. The early intermediates I_0 and $I_0^{\ddagger}$ have lifetimes in the picosecond time range and red-shifted absorption maxima (∼510 nm) (*10*, *11*). They decay to I_1, which has an absorption maximum at 465 nm and has the chromophore in a cis orientation through a rotation of its C9 carbonyl (*12*). In about 120 μs, this intermediate decays into I_2, in which the chromophore ring has moved out toward the solvent and becomes protonated (lifetime of ∼1.5 ms). A conformational change, which involves exposure of a significant part of the hydrophobic protein interior, forms the I_2' intermediate. Finally, I_2'

* To whom correspondence should be addressed. Tel.: 09/2645109. Fax: 09/2645338. E-mail: Jozef.Vanbeeumen@UGent.be.

‡ Ghent University.

§ University of Arizona.

[1] Abbreviations: PYP, photoactive yellow protein; Hh, *Halorhodospira halophila*; Sr, *Salinibacter ruber*; Rc, *Rhodobacter capsulatus*; Ppr, PYP-phytochrome related protein; WT, wild-type.

10.1021/bi701486n CCC: $40.75
Published on Web 01/17/2008

recovers back to the ground state in milliseconds (*13*). Since the I_2' intermediate is the longest living species and the only one with a significant conformational change, it is generally thought to be the signaling state of PYP.

There is only one instance where the functional role of PYP is clearly defined. In *Rhodocista centenaria* (formerly *Rhodospirillum centenum*), there is evidence that the hybrid photoreceptor Ppr, which has a PYP domain linked to bacteriophytochrome and histidine kinase domains, is involved in regulating the expression of a polyketide synthase related to chalcone synthase (*14*). It has recently been shown that blue-light activated PYP, in Ppr, functions to accelerate the recovery of the red-light activated phytochrome domain to the dark-adapted state (*15*). Moreover, expression of the polyketide synthase appears to be linked to the formation of desiccation-resistant cysts (*16*) that result from nutrient limitation and other stress, which could implicate a role for Ppr in regulating cyst formation. By way of contrast, PYP in Hh is proposed to be involved in mediating a photophobic response to blue light to avoid UV-radiation damage. The wavelength dependence of this response coincides with the PYP absorption spectrum, suggesting that PYP is the primary photoreceptor for this behavior (*17*); however, no conclusive evidence, such as the existence of gene inactivation mutants, has been presented yet.

As new genes encoding PYPs are discovered through genome sequencing, it becomes more obvious that those forms of PYP having significant differences in physical−chemical properties serve different functional roles (*6*). The diversity of PYP gene distribution has increased even more by the recent observation that PYPs can originate from non-phototrophic bacteria (i.e., *Idiomarina loihiensis* (*18*), *Burkholderia phytofirmans* (Joint Genome Institute), *Stigmatella aurantiaca* (The Institute for Genome Research), and Sr (*19*)), as well as from phototrophs.

Sr is a red, obligately aerobic, chemoorganotrophic, extremely halophilic bacterium. The species occupies the same habitat as *Halobacterium* and *Halorhodospira* species and was recently isolated from salt evaporation ponds in Spain (*20*). It grows at an optimal salt concentration of 20−30% and a temperature of 37−47 °C. The 16S rRNA sequence indicates that it is not an archaebacterium but that it is related to the *Cytophaga*−*Flavobacterium* branch of bacteria. Nevertheless, Sr has remarkable physiological similarities to the extremely halophilic *Halobacterium*. Like the latter, Sr has adapted its life at high salt concentrations by accumulating KCl in molar concentrations to provide the necessary osmotic balance (*21*). This greatly differs from the more common strategy used by all other known halophilic and halotolerant bacteria by which organic compatible solutes, such as ectoine, glycine betaine, and others, are produced and/or accumulated to respond to osmotic stress following the initial response, which involves a transient moderate increase in KCl (*22*).

We present here the first characterization of PYP from Sr. Although it has interesting differences that allow adaptation to the specific physiology of the organism, there are also similarities to the prototypic Hh PYP. The genetic context and the presumed function are also discussed.

MATERIALS AND METHODS

Cloning of Sr pyp. A polymerase chain reaction (PCR) was performed to amplify DNA encoding the Sr *pyp* (SRU_2224) using the Easy-A High Fidelity PCR cloning enzyme (Stratagene). PCR was performed according to the manufacturer's instructions and using Sr chromosomal DNA as a template. The following primers were designed based on the Sr genome sequence (*19*): 5′-GGAATTCCATATG-GCTGACTCTCAGGAATCCG-3′ and 5′-CATGCCTC-GAGTCACCGCTTCTGAATCAGGATCC-3′. The primers were designed with restriction sites for NdeI and XhoI, respectively (underlined in the sequence). The expression vector was constructed by ligating the NdeI/XhoI digested *pyp* fragment in pET20b (Novagen) digested with the same restriction enzymes. The construction of the pACYC(*tal*;*pcl*) plasmid that contains the two biosynthetic genes from Rc for holo-PYP formation was described earlier (*23*).

Overproduction and Purification of Sr PYP. All expression experiments were performed with *Escherichia coli* BL-21 (DE3). After co-transformation of pET20b(*Srpyp*) and pACYC(*tal*;*pcl*) to the bacterial cells, cultures were grown on carbenicillin (Cb, 100 μg/mL) and chloramphenicol (Cm, 25 μg/mL) antibiotics. An overnight culture was used to inoculate LB medium containing both antibiotics. The culture was grown at 37 °C until an OD_{600} of approximately 0.6. At that point, the temperature was lowered to 28 °C, and the cells were induced with a final concentration of 0.5 mM IPTG. The cells were pelleted by ultracentrifugation after 16 h of induction. After resuspending in Tris-HCl buffer (100 mM, pH 8.0), the cells were frozen at −20 °C until further purification. The cells were fractionated by sonication, followed by centrifugation to remove the cell debris. The soluble fractions were loaded onto a 10 mL Q-Sepharose Fast Flow column (Amersham Biosciences). Tris-HCl buffer (100 mM, pH 8.0) was used to apply the sample, and proteins were eluted using the same buffer supplemented with an increasing amount of NaCl (with steps of 100, 250, 350, and 500 mM and 1 M). The PYP eluted mainly with 350 mM NaCl. The yellow fractions were pooled and concentrated on Vivaspin 15R centrifugal filters (5000 MWCO, Sartorius). The purification was continued by size-exclusion chromatography on a Superdex 75 column (Hiload 16/60, Amersham Biosciences) with 100 mM Tris-HCl, pH 8.0, supplemented with 50 mM NaCl as the running buffer using an ÄKTA Explorer FPLC system (Amersham Biosciences). During this step, the holo-protein eluted in two separate peaks, of which the ratio between the first and the second peak was calculated to be 2.5 according to the absorbance at 431 nm. In fact, comparing the elution volume to a calibration curve indicated a dimeric and monomeric Sr PYP form present on the size-exclusion column. Mass spectrometry identified the monomeric peak as a PYP variant that was N-terminally truncated by 30 amino acids as compared to the dimeric peak, representing full-length Sr PYP. This observation suggests that the N-terminal extension induces dimerization of the native form. After this step, SDS-PAGE analysis showed that the sample was >90%, pure, but the UV−vis absorption spectrum showed a 280/431 nm ratio of 1.2, as the consequence of the presence of apo-PYP (i.e., PYP protein lacking a chromophore). Holo- and apo-PYP were partially separated using hydrophobic interaction chromatography on

a Phenyl Sepharose CL-4B column (GE Healthcare). Sr PYP was applied to the column in 50 mM Tris-HCl as a binding buffer, pH 8.0, supplemented with 1.7 M $(NH_4)_2SO_4$, and elution was performed with the same buffer without salt using a linear gradient. After this step, the 280/431 ratio of holo-PYP was 0.94, with a yield of 1.5 mg of full-length native PYP per liter of culture.

Mass Spectrometry. Molecular mass analysis was performed on a Q-TOF mass spectrometer (Micromass) equipped with a Nanomate 100 (Advion) electrospray source. Approximately 5−10 pmol of protein was dissolved in 5 μL of 50% ACN/0.1% HCOOH and infused into the ESI-chip.

To localize the cleavage site of the truncated PYP form, the holo-protein was digested with trypsin, in 50 mM NH_4HCO_3, for 6 h at 37 °C. The ratio of trypsin to holo-protein was 1:100 (w/w). The resulting peptides were analyzed by MALDI-TOF/TOF mass spectrometry on a 4700 Proteomics Analyzer (Applied Biosystems).

UV−Vis Spectroscopy and Time-Resolved Laser Spectroscopy. Absorption spectra were obtained using a UVIKON spectrophotometer (Kontron). Samples were measured using Tris buffer at varying concentrations and values of pH, as indicated. The recovery experiments with Sr PYP were carried out in universal buffer (2 mM CAPS, CHES, Bicine, HEPES, PIPES, MES, and sodium citrate) or Tris buffer, as indicated. The protein was first bleached by a 0.5−1 min exposure to a tungsten lamp (60 W), and the recovery was subsequently measured in the dark in the spectrophotometer. The maximum bleach was achieved after ~3 min illumination. Absorbance changes were measured over a maximal 250 min time range, and the kinetic data were fit using Sigmaplot 8.0 software. The laser flash apparatus and data analysis protocol to study the microsecond time recovery were as described previously (*8*, *24*).

Fluorescence Spectroscopy. Fluorescence excitation and emission spectra were recorded on a PC1 photon counting spectrofluorometer (ISS), and the data were analyzed with the VINCI software. The samples for fluorescence measurement were in 50 mM Tris-HCl, pH 7.1, and had an absorbance of 0.12 at their maximum wavelength (431 nm for Sr PYP and 446 nm for Hh PYP).

RESULTS AND DISCUSSION

Gene Context of Sr PYP. The completed genome sequence of Sr (*19*) contains one gene coding for a PYP. To date, it is the only example of a *pyp* gene being discovered outside the proteobacteria, and it is one out of four instances in which it has been found in a non-photosynthetic species. In none of these cases has the PYP protein been characterized. Five of the 13 species in which PYP has been identified are halophiles, suggesting that PYP may be involved in the regulation of osmotic pressure. However, the gene for PYP (SRU_2224) is surrounded by a number of hypothetical proteins, which complicates the inference of a possible functional role based on the nature of the genetic context. There are no obvious regulatory genes in the vicinity of PYP with which it may interact, but there are genes for transporters and porins in the near distance that may be relevant to its function. Adjacent to PYP is an operon consisting of a hypothetical protein (SRU_2223) and a membrane protein of the TerC family (SRU_2222, for Tellurite resistance) which is divergently transcribed relative to the *pyp* gene. Converging on *pyp* from the downstream side, the gene for a membrane protein (SRU_2225) is divergently transcribed with a hypothetical protein (SRU_2226) and a homologue of UbiE, an *S*-adenosyl methionine dependent methylase (SRU_2227). None of these nearby genes have obvious relevance to the possible function of PYP.

Further downstream, however, there are two stomatin homologues (SRU_2228 and SRU_2229) and an associated protease (SRU_2230). When cleaved by the protease, stomatin functions to open ion channels and regulate transporters (*25*). More generally, these proteins function to degrade membrane proteins that are not folded properly. Six genes further downstream is an *ompA* porin homologue (SRU_2237) followed by a sulfate transporter (SRU_2239). A 19-gene hyper-salinity island including six genes for potassium uptake and five genes for cationic amino acid transporters was identified 32 genes downstream of *pyp* (*19*). Immediately preceding it is a potassium/proton antiporter. All these data suggest that the hypersalinity island may be larger than thought and may include PYP and the intervening genes. Thus, Sr PYP may be loosely associated with porin and transporter genes. Nevertheless, we were unable to locate any sensor kinase or regulator between PYP and the end of the hypersalinity island that might act as a reaction partner for PYP.

In Hh, the two biosynthetic enzyme genes, a tyrosine ammonia lyase and a *p*-hydroxycinnamoyl:CoA ligase (*23*), are located adjacent to that for PYP. In Sr, two ammonia lyase genes, SRU_717 and SRU_722, are present 1.8 Mbp from the *pyp* gene and mutually separated by 6 kbp. SRU_717 has an H103L104 sequence equivalent to the *Rhodobacter sphaeroides* active site residues H89L90 that determine tyrosine ammonia lyase specificity (*26*). SRU_722, on the other hand, is consistent with having histidine ammonia lyase activity. We thus believe that SRU_717 is the biosynthetic enzyme for PYP. The second biosynthetic enzyme, *p*-hydroxy-cinnamic acid:CoA ligase, is less conserved than are the tyrosine ammonia lyases. Nevertheless, we found weak homology in SRU_1355, annotated as an *o*-succinyl-benzoate:CoA ligase that has most of the active site residues found in the 4-chloro-benzoate:CoA ligase of which the 3-D structure has been determined (*27*). There is little doubt that SRU_1355 codes for a CoA ligase, but the substrate specificity is less certain.

Sequence Homology. Figure 1 shows the sequence alignment of Sr PYP with the prototypic PYP from Hh BN9626. Sr PYP consists of 156 amino acids and shows only 37% sequence identity with 46 identical amino acids, but all amino acids previously identified as necessary for spectral tuning of the chromophore are present, except for the equivalent of Hh T50 and R52. The former is conservatively substituted by serine in Sr PYP, as in *R. centenaria* Ppr, but R52 is replaced by isoleucine, which may have functional consequences because it must move out of the way of the chromophore during isomerization (*28*).

Sr PYP has an N-terminal extension with 32 additional amino acids as compared to Hh PYP and is the most acidic PYP species known to date, with a theoretical pI value of 3.95, and it remains acidic when the 32 amino acid extension is omitted from the calculation (theoretical pI value is 4.2). This extremely acidic nature of Sr PYP is consistent with

```
Hh BN9626       ------------------------------ -MEHVAFGSEDIENTLAKMDDGQLDGLAF 28
Sr              MADSQNPYSYLREDDPDSAPGDSGDADEPEP^PATDLAFDDEGVGEELRHVDEDELNAAPF 60

Hh BN9626       GAIQLDGDGNILQYNAAEGDITGRDPQEVIGKNFFKDVAPCTDSPEFYGKFKEGVASGNL 88
Sr              GIIQIDDAGVVQFYNRYESNLSGIDPADAVGANFFTELAPCSNNPLFFGRFKDGVREGGL 120
                              42   46    50 52                69

Hh BN9626       NTMFEYTFDYQMTPTKVKVHMKKALSGDSYWVFVKRV 125
Sr              DEYFTYTFTYQMRPTLVDVRLYRDEAEN-NWILIQKR 156
                        98 100
```

FIGURE 1: Sequence alignment of the photoactive yellow proteins from Hh (BN9626) and Sr. The conserved residues are indicated in bold. Met100 and the residues involved in chromophore binding through a hydrogen-bonding network are marked in gray. The conserved Cys69, which forms a thioester bond with the chromophore, is marked in black. The numbering of the important residues is according to Hh PYP. The cleavage site of Δ31-PYP is also indicated (^).

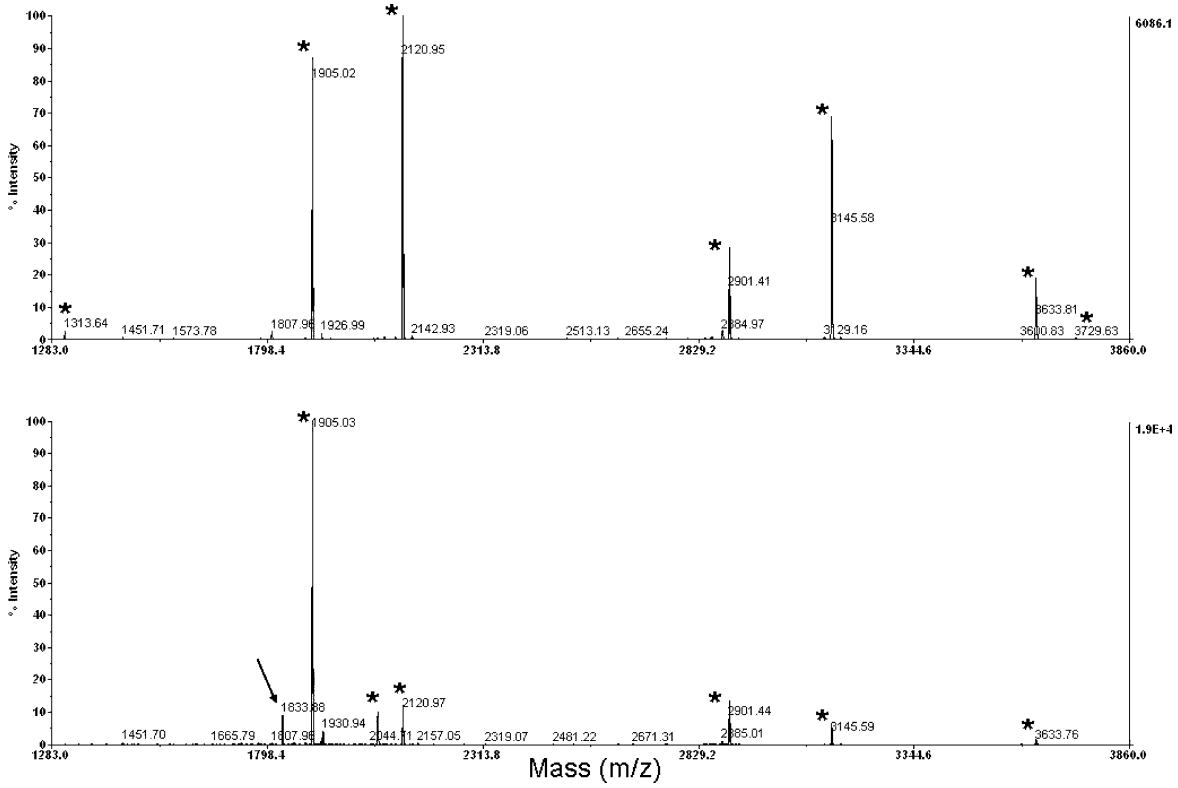

FIGURE 2: Comparative peptide mass fingerprint (PMF) of Sr PYP (upper trace) and Δ31-PYP (lower trace) after trypsin digest. The mass peaks corresponding to tryptic peptides are marked with an asterisk (∗) and listed in Table 1. A peak with a mass of 1833.88 Da, corresponding to the theoretical mass of peptide Pro 32−Arg 48, is indicated by the arrow.

the high intracellular potassium concentration as a mode of haloadaptation. To ensure protein solubility at such a high ionic strength, *Salinibacter* proteins have a high content of acidic amino acids and a relatively low content of hydrophobic residues (*19*, *29*).

Protein Production, Purification, and Mass Spectrometry. To determine as to whether the Sr *pyp* gene encodes a functional protein and to study its properties, we cloned and expressed the PYP coding gene in *E. coli*, along with the two biosynthetic enzyme genes from *R. capsulatus* (i.e., *pcl* and *tal*). The holoprotein was successfully produced and purified, indicating that Sr *pyp* is not a pseudo-gene. The electrospray mass spectrum of purified Sr PYP yielded masses of 17 402 and 17 547 Da, corresponding to the calculated masses of apo- and holo-Sr PYP protein, respectively, both without the N-terminal methionine (data not shown). The apo-/holo-protein ratio was calculated to be 1:3 according to the height of their respective mass peaks. During purification, it became clear that native Sr PYP behaved as a dimer during size-exclusion chromatography, while a second form (with a relative abundance of 40% as compared to the full form) eluted as a monomer and showed molecular masses of 14 210 and 14 355 Da by ESI-MS. These masses correspond to the calculated masses of truncated apo- and holo-Sr PYP protein, respectively, both lacking the first 31 N-terminal amino acids (including the initiator Met). The cleavage site of the truncated Sr PYP form (Δ31-PYP) is located at the C-terminal side of proline 31, as confirmed by MALDI-MS of a tryptic digest. The peptide mass fingerprint of Δ31-PYP showed the absence of two peaks of masses 1313.63 and 3729.63 Da, corresponding to the respective peptides Ala 2−Arg 12 and Glu 13−Arg 48. Instead, a new peak with a mass of 1833.88 Da occurred, which corresponds to the theoretical mass of peptide Pro 32−Arg 48, as shown in Figure 2 and listed in Table 1. Since the intracellular salt concentration in Sr is unusually high to regulate osmotic balance, we performed a size-exclusion chromatography experiment with the full-length SrPYP form using 100 mM Tris-HCl, pH 8.0, supplemented with 1 M KCl as the running buffer. The dimer was not interrupted and therefore

is likely to be physiological. The cleavage of a Pro−Pro bond is rather unusual, and it may be significant that the protein is partially cleaved by proteolysis during production and purification close to the start of the homology with Hh PYP, as shown in Figure 1. This suggests that the 32 residue extension is disordered relative to the remainder of the protein and, based on its behavior during size-exclusion chromatography, induces dimerization of the full-length Sr PYP form. Dimerization of Sr PYP is unique, as no precedents with any of the other published PYPs have been described before. However, it is not uncommon for photoreceptor proteins to form functional dimers. For example, plant phytochromes exist as red-light sensing homodimers (*30*), which is also the case for the blue-light absorbing *Arabidopsis* cryptochrome 1 (CRY1), where homodimerization of the N-terminal domain has been shown to be essential for photoreceptor activity (*31*). Another example of a dimeric photoreceptor is the blue-light sensing BLUF domain of the transcriptional anti-repressor AppA. In the dark state, dimerization is mediated through hydrophobic interactions between a β-sheet of two monomers, as shown by X-ray crystallography (*32*, *33*).

In Hh PYP, the N-terminal cap, which consists of a helix-turn-helix motif, is believed to have a role in signal transduction (*34*, *35*). However, no structural motif could be predicted for the N-terminal extension of Sr PYP, using secondary structure prediction tools (i.e., Predator (*36*)). Moreover, a Psi-Blast with the 32 amino acid containing N-terminal sequence does not find any significant homology with protein entries in the database that would provide any hint as to function. Thus, although the truncation of the N-terminal extension does not seem to influence the photochemical properties (as further described below), its implication in signaling remains speculative as no homologous precedents are available.

UV−Vis Spectroscopy. Effects of Chaotropic and Kosmotropic Agents and Temperature on Full-Length SrPYP. As compared to known PYPs, Sr PYP has a blue-shifted absorption maximum at 431 nm and a broader peak as the result of a blue spectral shoulder (Figure 3a, solid line). The absorption maximum can be partially bleached by room light and to a greater extent by white-light illumination from a 60 W tungsten source, as also shown in Figure 3a. The spectral changes are completely reversible by overnight incubation in the dark. The light minus dark difference spectrum (Figure 3b) shows the formation of an intermediate similar to Hh PYP I_2, with a 334 nm maximum and an isosbestic point at 361 nm, although somewhat blue-shifted as discussed below. There is also evidence for an equilibrium with a small amount of the earlier intermediate I_1, in that there is a small but broad difference peak in the vicinity of 490 nm.

The absorption spectrum of Sr PYP suggests the presence of an intermediate spectral form similar to that of the Y42F mutant of Hh PYP (*37*, *38*) and WT Rc PYP (*39*). In the Y42F mutant, a 390 nm spectral shoulder on the 458 nm maximum, due to a second less stable chromophore conformation in the ground state, was found to be pH and temperature dependent and to be strongly affected by the opposing effects of chaotropes and kosmotropes (*37*). This intermediate spectral form, the hallmark of which is a wavelength maximum that is dependent upon environmental

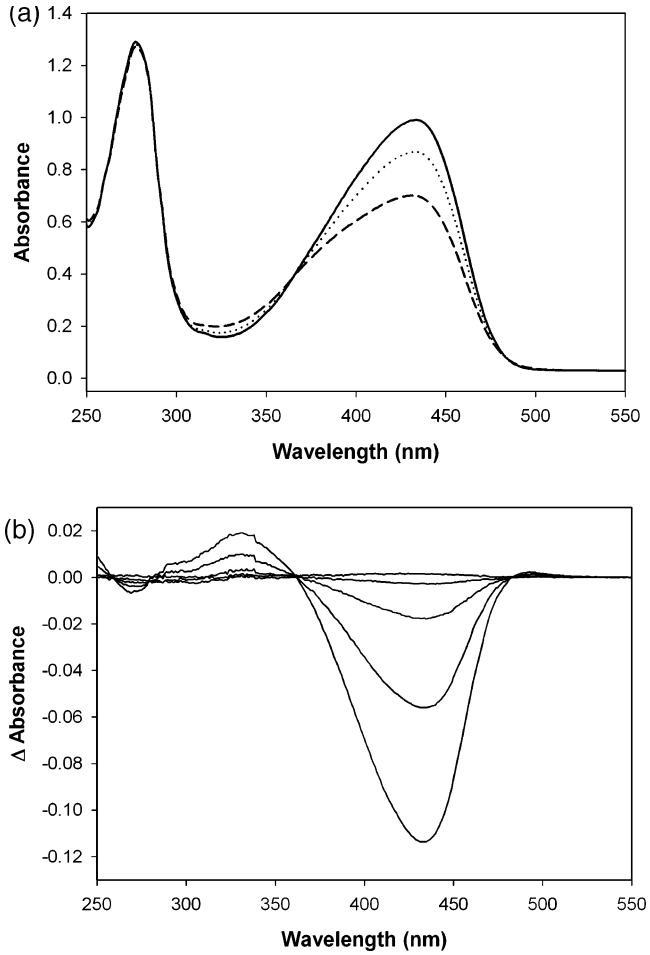

FIGURE 3: Effect of light on the spectrum of Sr PYP in 50 mM Tris, pH 7.5. (a) Dark-adapted spectrum (solid line) and spectra following exposure of room light (dotted line) or 1 min illumination from a tungsten source (dashed line). (b) Light minus dark difference spectrum for Sr PYP recovery in 50 mM Tris-HCl, pH 8, at room temperature. Spectra were taken at different time points after illumination with a tungsten source. The isosbestic point for the 334 to 446 nm transition is at 361 nm.

factors, was later found in other PYP mutants and has been ascribed to a PYP form with a higher and continuously variable dielectric constant and altered hydrogen bonding to E46 in the chromophore region (*38*). Rc PYP displays a secondary peak at 375 nm that is also temperature and pH dependent, although there is an additional PYP form present that has the chromophore in a cis conformation (with a presumed maximum close to 350 nm) that is stabilized at low temperature, which complicates interpretation of the temperature dependence (*39*). To investigate as to whether a similar behavior occurs in Sr PYP and to further characterize the spectral shoulder, we studied the effects of chaotropic and kosmotropic agents, as well as temperature.

The effects of the kosmotrope $(NH_4)_2SO_4$ and chaotrope NH_4Cl are shown in Figure 4a,b, respectively. Surprisingly, like KCl, both ammonium salts stabilize the main peak at 431 nm by significantly increasing the absorption maximum while the blue shoulder decreases accordingly. Therefore, Sr PYP appears to respond more strongly to ionic strength than to specific ion effects. We conclude that the shoulder on the short wavelength side of the absorption maximum in Sr PYP is due to a less stable conformation that is eliminated at high ionic strength. However, we have insufficient data

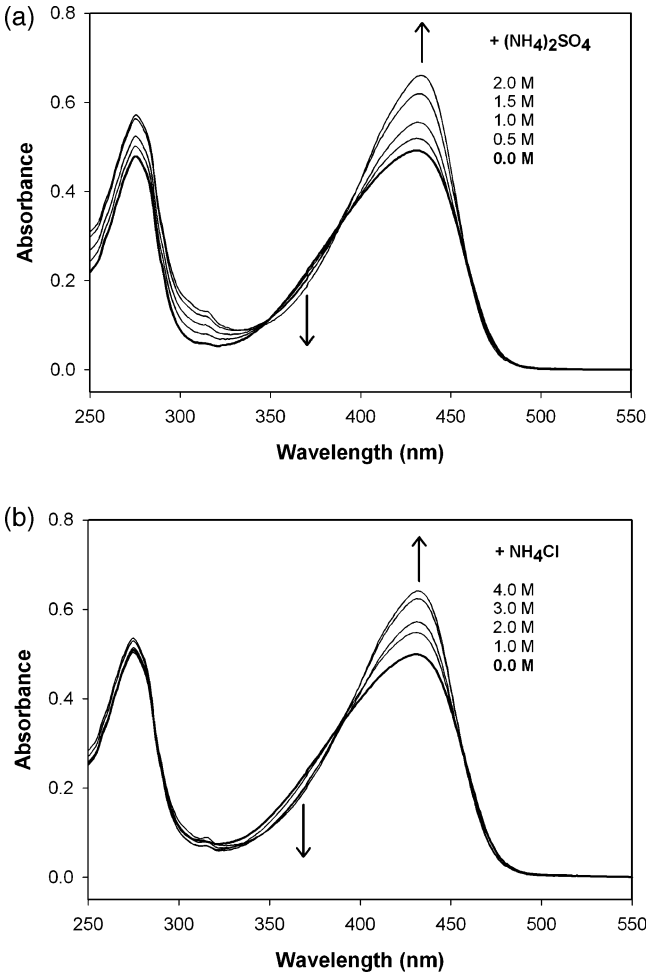

FIGURE 4: (a) Effect of increasing concentrations of the kosmotrope $(NH_4)_2SO_4$ and (b) increasing concentrations of the chaotrope NH_4-Cl on the absorption spectrum of Sr PYP in 50 mM Tris-HCl buffer, pH 7.5, at room temperature. The arrows indicate the direction of increasing salt concentration.

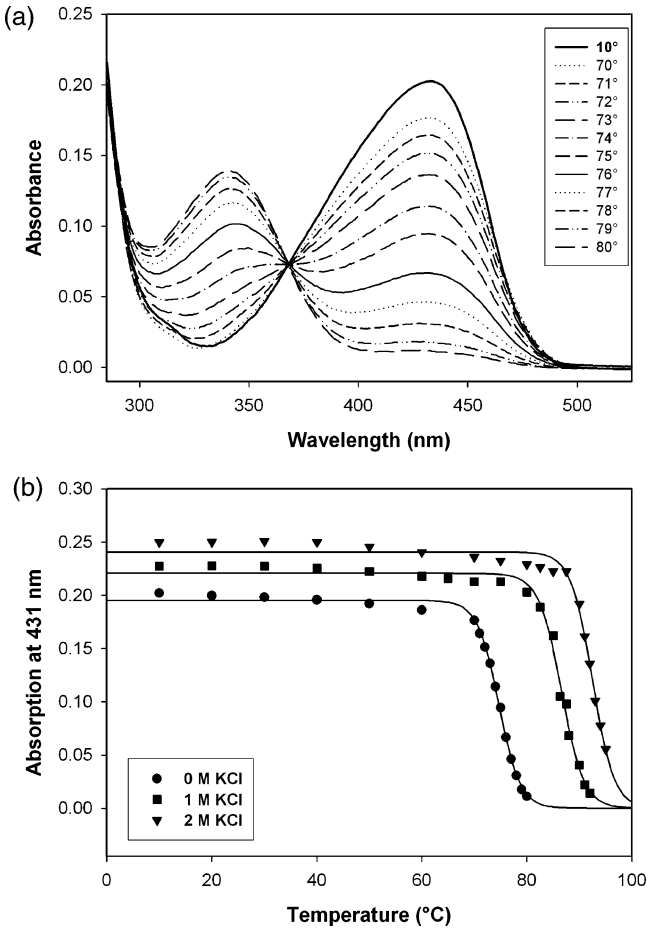

FIGURE 5: (a) Temperature dependence of the absorption spectrum of Sr PYP in 50 mM TrisHCl, pH 7.5. Sr PYP can be reversibly heated to 80 °C, at which the 431 nm peak is converted to a denatured 340 nm species with a single isosbestic point. (b) UV−vis absorbance at the 431 nm wavelength maximum as a function of temperature in the absence (circles) and presence of 1 M (squares) and 2 M (triangles) KCl. The solid lines represent the fitted curves.

to say as to whether it has the same origin as in Hh PYP Y42F or in WT Rc PYP.

Sr PYP can be reversibly heated to 80 °C as shown in Figure 5a. However, the absorbance at 431 nm slightly drops prior to denaturation as shown by the 431 nm absorbance versus temperature plot in Figure 5b. The 10° minus 70° difference spectrum (data not shown) indicates that the spectral shoulder is increased relative to the 431 nm maximum before it denatures. Under the low ionic strength conditions of measurement (50 mM Tris-HCl, pH 7.5), the melting temperature T_m is 74 °C, which is intermediate between that of WT Hh PYP (82 °C) and the Y42F mutant (65 °C) (*38*). However, addition of KCl, of which Sr cells contain molar amounts to regulate osmotic balance, increases the melting temperature to 86.6 and 92.5 °C with 1 and 2 M KCl, respectively, as shown in Figure 5b. This indicates a stabilizing effect of KCl on the native protein conformation. The relatively high melting temperature suggests that Sr PYP is somewhat less stable than Hh PYP under low ionic strength conditions but may be more stable at high ionic strength (although Hh PYP was not studied under these conditions).

Fluorescence Spectroscopy. We examined the fluorescence excitation spectrum (with emission monitored at 490 nm) and the emission spectrum (with excitation at 400 nm), as

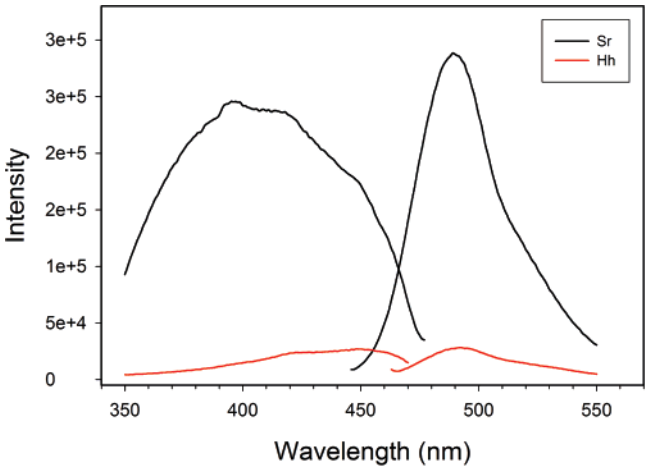

FIGURE 6: Fluorescence excitation and emission spectra of Sr PYP (black) and Hh PYP (red) in 50 mM Tris-HCl, pH 7.1. Sample absorbance was 0.12 at their maximum wavelength (431 nm for Sr PYP and 446 nm for Hh PYP).

shown in Figure 6. As a control, we also measured the Hh PYP fluorescence spectra. It had previously been shown that the Hh PYP fluorescence quantum yield is relatively low (~0.2% (*40*)). The excitation maximum of Sr PYP fluorescence appears to be around 400 nm, which corresponds better

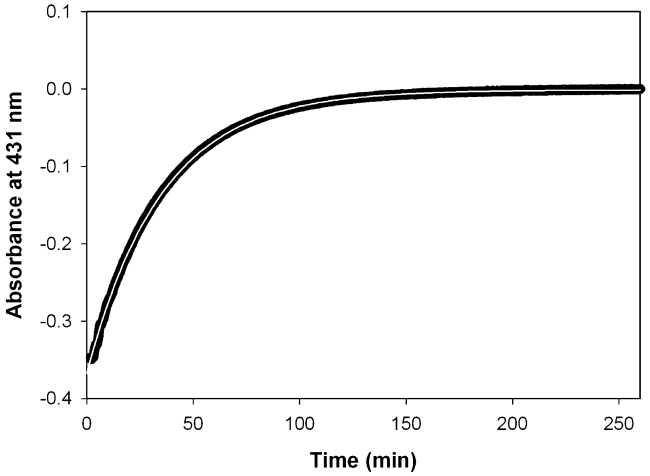

FIGURE 7: Kinetics of dark recovery of Sr PYP in 50 mM Tris-HCl, pH 7.5, after 1 min of illumination with white light. The solid white line represents a fitted curve to the data.

to the spectral shoulder in the UV−vis absorption spectrum than to the 431 nm maximum. It is, therefore, likely that the spectral shoulder is the basis for the high Sr PYP fluorescence. The fluorescence emission maximum of Sr PYP is at 490 nm, as compared to 495 nm for Hh PYP, and the intensity is about 10-fold higher than for Hh PYP when measured with the equivalent visible absorption. Taking into account that the absorption maximum of Sr PYP is blue-shifted by 15 nm (431 nm vs 446 nm), the fluorescence maximum is less blue-shifted (only 5 nm), as compared to the expected value. If indeed the spectral shoulder is the fluorescent form, then this red-shift would be expected to be even larger. We recently showed that the Hh mutant Y98Q also has an increased and red-shifted fluorescence (*41*). On the basis of structural data, it was concluded that the red-shift in fluorescence was due to an increase in polarity in the chromophore environment, which was caused by a repositioning of R52 in the ground state, allowing two water molecules to come in close proximity of the chromophore. Since Sr PYP has a natural R52I substitution, it may likewise cause a change in dielectric constant of the chromophore surroundings by making it more solvent accessible, leading to the observed red-shifting effect on the fluorescence.

The excitation spectrum reveals that there is not only a shift in fluorescence of Sr PYP under UV-illumination, but also a higher intensity, similar to Hh mutant Y42F. Structural analysis of Y42F indicates possible chromophore bowing to be responsible for the control of chromophore fluorescence (*42*). In WT Hh PYP, chromophore fluorescence is suppressed by the intramolecular forces in the folded protein that are responsible for spectral tuning of the chromophore. Our fluorescence results indicate that the spectral shoulder is causing the increase and shift in fluorescence and, therefore, is likely to have the chromophore in a different conformation and a more hydrophilic environment.

Recovery Kinetics. Effects of KCl, Alcohols, Temperature, and pH. We determined the kinetics of recovery of Sr PYP following white-light photoactivation, which is shown in Figure 7. The rate constant at pH 7.5 (4.27×10^{-4} s^{-1}) indicates a 14 000-fold slower recovery for Sr PYP as compared to Hh PYP (6.0 s^{-1}) at the same pH value. Since we could only bleach 37% of the 431 nm absorbance peak (Figure 3a), we investigated the possibility of a biphasic

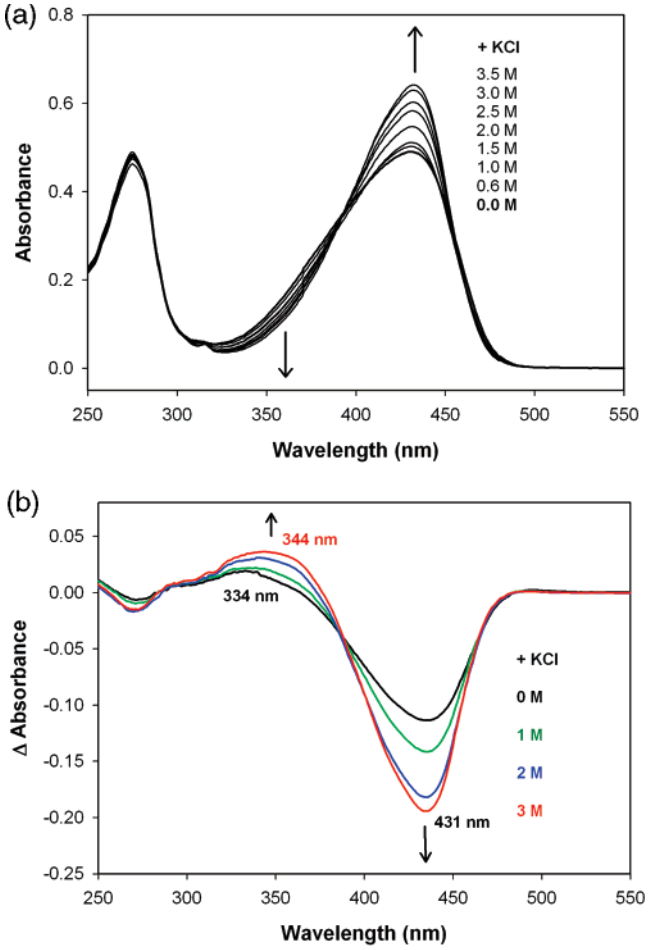

FIGURE 8: (a) Effect of increasing concentrations of KCl on the absorption spectrum of Sr PYP in 50 mM Tris-HCl, pH 7.5, at room temperature. The arrows indicate the direction of increasing salt concentration. (b) Effect of increasing concentrations of KCl on the light minus dark difference spectra, as indicated by the arrows.

recovery with a fast and a slow phase. However, no fast recovery was observed within the limit of detection of our laser equipment (microsecond time range). An alternative explanation for the low amplitude of bleach is the competition between photobleach and photoreversal. However, we observed the same effect with blue light (>390 and <510 nm) that does not illuminate I_2 or I_2'. It is also possible that there is a significant amount of the I_1 intermediate present in equilibrium with I_2 following illumination, as suggested by the 490 nm peak in the difference spectrum (Figure 3b). In Hh PYP, the absolute spectrum of I_1 is somewhat red-shifted relative to the ground state but has about half the intensity (*43*), consistent with this explanation. The residual absorbance after maximum bleach has shifted to 429 nm, and there is relatively more of the spectral shoulder (Figure 3a, dashed line). This suggests that the contribution of I_1 is relatively small (otherwise, the maximum would be red-shifted as in Hh PYP). Although there is no precedent for it, I_1 does not have to be red-shifted in Sr PYP but could be broadened instead. Since the spectral shoulder is increasing relative to the 431 nm form, it appears as if this form is not photoactive. In addition, when the sample is bleached in 3 M KCl, where there is an increase in 431 nm absorbance due to conversion of the spectral shoulder (Figure 8), there is at least 10% more photobleach of the sample. Figure 8b

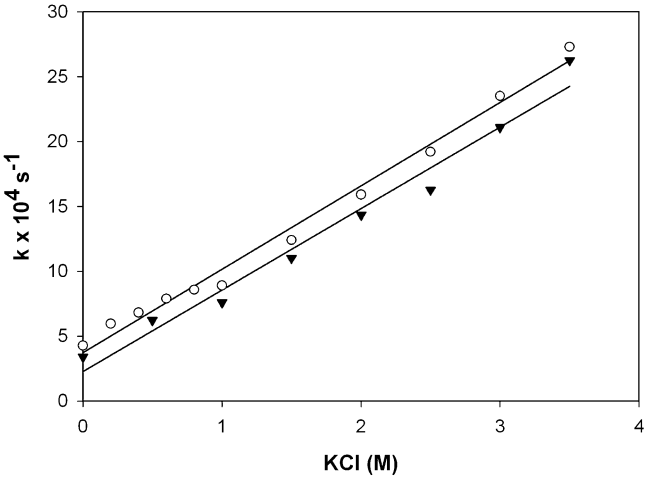

FIGURE 9: Effect of increasing concentrations of KCl on the recovery rate of Sr PYP (open circles) and Δ31-PYP (triangles) in 50 mM Tris-HCl, pH 7.5, at room temperature.

in comparison with Figure 8a shows that the relative amount of bleach has increased from 37 to 47% by increasing the KCl concentration from 0 to 3 M. As far as our data allow us to conclude, it appears that a combination of the presence of I_1 and the residual spectral shoulder is presumably the explanation for the maximum bleach of only 37% at 431 nm.

As noted before, the physiological intracellular salt concentration in Sr is unusually high, as the organism maintains a high concentration of potassium inside its cytoplasm, keeping an osmotic balance against the high sodium chloride concentration outside (the species will not grow at less than 15% salt in the medium). Although procedures to establish intracellular ion concentrations suffer from certain artifacts, such as the possibility of leakage of ions from the cells during cell preparation, estimated intracellular KCl concentrations range from 1 to 4 M (*21*). Therefore, we analyzed the spectrum and kinetics of Sr PYP in high concentrations of KCl as shown in Figures 8a and 9, respectively. An increasing amount of KCl influences the 431 nm absorption peak and the intermediate spectral form in the same manner as observed with the kosmotrope $(NH_4)_2SO_4$ and the chaotrope NH_4Cl, which further points to a general ionic strength effect.

In addition, the recovery rate of Sr PYP following white-light photoactivation is significantly affected by KCl. The rate constant increases almost linearly with increasing amounts of KCl, as shown in Figure 9. In the 0−3.5 M salt range, Sr PYP recovers approximately 6.4 times faster, but the maximum recovery observed (at 3.5 M KCl) is still 2200 times slower than for Hh PYP without salt and at the same pH value. Although Hh, like Sr, is an extreme halophile, it accumulates ectoine and betaine rather than KCl. Recovery of Hh PYP shows a different effect of ionic strength, first decreasing due to screening of the ion pair E12/K110 (below 600 mM) and then increasing at higher ionic strength (*44*). The sequence alignment shows that the ion pair between E12 and K110 is absent in Sr PYP. This is consistent with the lack of initial decrease in the rate constant at low salt concentration.

It is possible that the I_2/I_2' equilibrium in Sr PYP is shifted toward I_2 in high salt concentrations. A similar effect was observed in Hh PYP and was explained as the stabilizing effect on the compact and folded structure of I_2 (*44*). Comparing the difference spectrum of Sr PYP after illumination in high salt concentrations with that without salt indicates that there is a less UV-shifted absorbance maximum (344 nm vs 334 nm) (Figure 8b). However, the intermediate spectral form disappears at high ionic strength, which influences the apparent wavelength maximum for I_2. Thus, on the basis of the difference spectrum alone, we cannot say as to whether or not ionic strength affects the I_2/I_2' equilibrium as it does in Hh PYP.

Although we have shown that the I_1 and I_2 intermediates may be present in Sr PYP, we have not yet demonstrated the presence of I_2', which is characterized in Hh PYP by a conformational change that exposes a hydrophobic site to solvent. Direct measurements of I_2' are complicated by its low extinction coefficient, similar to I_2 (350 nm vs 370 nm in Hh PYP), and its intrinsic instability. However, aliphatic alcohols slow Hh PYP recovery, consistent with the bleached state being more hydrophobic than the ground state, due to a conformational change upon I_2' formation (*45*). We therefore studied the effect of alcohol on the recovery of Sr PYP and found that it is similar to that of Hh PYP, but only one-third the magnitude, as shown in Figure 10a. This suggests that the bleached state is less hydrophobic than in Hh PYP or that there is less I_2' being formed in Sr PYP, at least at high KCl concentrations (1 M).

An alternative indirect measurement of I_2' is through temperature dependence determination. The recovery of Hh PYP has a bell-shaped dependence on temperature (*45*): the reaction becomes only twice as fast between 5 and 35 °C and then becomes 3-fold slower up to 62 °C. This deviation is ascribed to a change in heat capacity of the protein as a result of the bleached state being more hydrophobic than the ground state (*46*). Unlike Hh PYP, the effect of temperature on the recovery of Sr PYP appears to show a normal Arrhenius behavior, with an activation energy of ∼62 kJ/mol in 1 M KCl. In the absence of salt, there is some curvature in the Arrhenius plot, consistent with the effect of alcohol (Figure 10b) and indicative of a smaller amount of I_2' than in Hh PYP. The heat capacity change for Sr PYP (−1.53 kJ/mol K) is only half of that in Hh PYP (−2.73 kJ/mol K). If the two highest temperature points are ignored in the high ionic strength plot, the remaining data show a curvature that, when fit (dashed line in Figure 10b), yields a heat capacity change of −0.75 kJ/mol K. As to whether or not there is curvature in the high ionic strength data, the conclusion remains that there is less I_2' formed than at low ionic strength.

The solution pH has a significant influence on the ground state recovery rate, as it is increased 17-fold between pH 4.5 and 9.0 in Sr PYP. The pH dependence is sigmoidal and has a single pK_a value at 5.8, as shown in Figure 11. In contrast, the recovery of Hh PYP is optimal at pH 8 and has a bell-shaped dependence on pH governed by pK_a values of 6.4 and 9.4, presumably due to E46 and the chromophore hydroxyl (*47*). Both the slow kinetics and the pH dependence of Sr PYP are more like the M100A mutant of Hh PYP (*48*), which indicates that the equivalent of M100 adopts a different conformation in Sr PYP, thereby preventing interaction with the chromophore and catalysis of recovery. This is similar to the *R. centenaria* PYP domain (*49*) and the Y98Q Hh

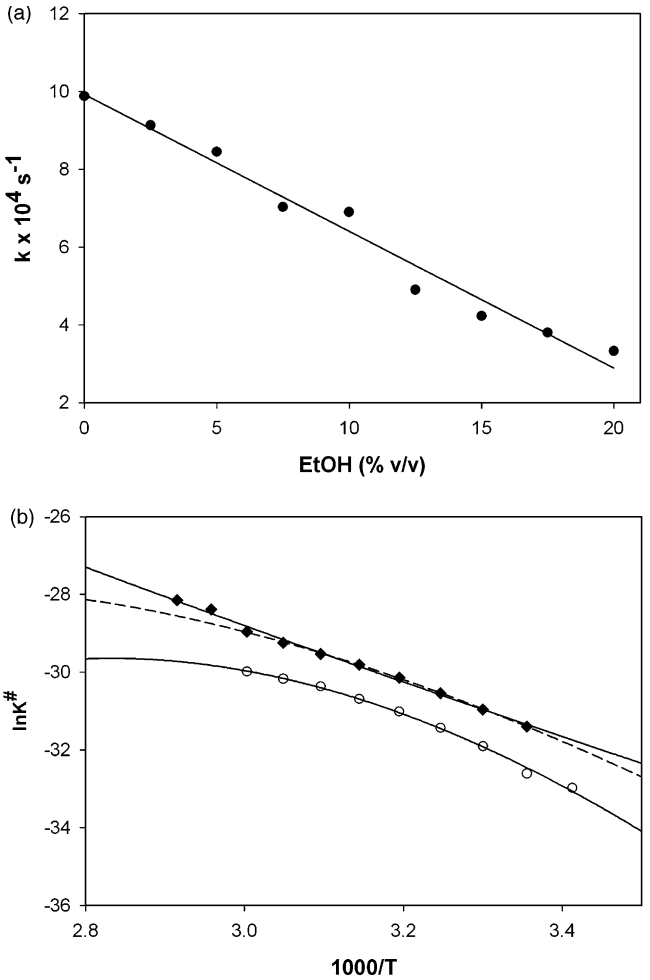

FIGURE 10: (a) Effect of EtOH/water mixtures on recovery kinetics after white-light illumination of Sr PYP in 50 mM Tris-HCl, pH 7.5, and 1 M KCl. (b) Temperature dependence of kinetics of recovery of Sr PYP in 50 mM Tris-HCl, pH 7.5, in the absence (open circles) and presence (filled diamonds) of 1 M KCl. The activation equilibrium constant $K^{\ddagger}$, calculated from the rate constant k using Van Brederode's equation (eq 12 in ref *46*) is shown as a function of temperature. The data were fitted using Van Brederode's equation (eq 13 in ref *46*).

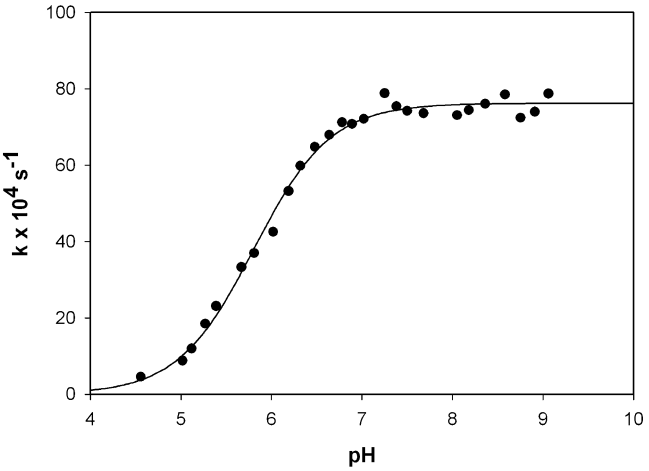

FIGURE 11: pH profile of the kinetics of recovery of Sr PYP at 37 °C in universal buffer supplemented with 2.5 M KCl. The solid line represents the fitted curve with a pK_a value of 5.8.

PYP (*41*). In addition, the Hh PYP M100A/R52A double mutant has a more pronounced pH dependence than the single mutant (*41*). This is presumably because R52 normally acts as a counterion for the chromophore in the bleached state (*28*). Because Sr PYP has a substitution of Ile for the equivalent of R52, we expected a similar pH dependence. There might still be a second pK_a value, similar to the one in M100A/R52A (pK_a = 10), but we were unable to measure it due to the hydrolysis of the chromophore above pH 9.4.

Table 1: Calculated and Experimentally Determined Masses of Tryptic Peptides of Heterologously Produced Sr PYP

peptide position	theoretical mass (Da)[a]	experimental mass (Da)
Ala 2−Arg 12	1313.39	1313.64
Glu 13−Arg 48	3729.53	3729.63
His 49−Arg 76	3145.52	3145.58
Tyr 77−Arg 110	3633.70[b]	3633.81
Glu 117−Arg 133	2121.31	2120.95
Glu 117−Arg 140	2901.38	2901.44
Leu 141−Lys 155	1904.99	1905.02
Leu 141−Arg 156	2061.09	2061.08
Pro 32−Arg 48	1833.93	1833.88

[a] Calculated using monoisotopic masses of the amino acids and giving peptide masses as $[M + H]^+$. [b] Mass without chromophore.

Spectrum and Kinetics of Δ31-PYP. The observed truncation of Sr PYP by 31 amino acids does not change the UV−vis absorption spectrum and has no significant effect on the ground state recovery after white-light illumination (calculated rate constant at pH 7.5 in 50 mM Tris-HCl is 3.4×10^{-4} s^{-1}) (data not shown). Moreover, the ground state recovery of Δ31-PYP is as strongly dependent on ionic strength as the unprocessed form, as shown in Figure 9. This argues against a functional role for the N-terminal extension, but in the absence of an interaction partner protein, a final conclusion is premature.

Other Photoreceptors in Sr. Although Sr is a non-photosynthetic organism, its natural habitat is the same as photosynthetic organisms such as *Halobacterium* and *Halorhodospira*. It is therefore likely to use similar photoreceptors for survival in these high light conditions. Besides a PYP coding gene, the *Salinibacter* genome also contains four bacterial rhodopsin genes and numerous chemotaxis genes that may point to a possible complex photobehavior for this extremely halophilic heterotroph. Three rhodopsin genes are related to *Halobacterium* rhodopsins and may have similar functions based on their genomic organization (*19*). One (SRU_2780) is a possible chloride pump, and another (SRU_1500) codes for a unique light-harvesting complex, called xanthorodopsin, that is shown to be a light-driven proton pump. Besides the retinal chromophore, it uses a carotenoid antenna (salinixanthin) to extend the absorption range beyond what is possible with retinal alone (*50*, *51*). The other two (SRU_2511 and SRU_2579) are predicted to be sensory rhodopsins (SR), distantly related to SRI. In *Halobacterium salinarum,* sensory rhodopsin I (∼587 nm) and sensory rhodopsin II (∼487 nm) interact with tightly bound transducer proteins to produce a color-sensitive phototactic behavior via a phosphorylation cascade modulating the cell's flagellar motor (*52*). Sr is also motile, and flagella have been observed through electron microscopy, although the number or localization could not be inferred (*20*). It is likely that SRU_2579 has a photosensory function as it is immediately followed by an Htr1 transducer (SRU_2258) as in *H. salinarum*. The best chances are that SRU_2579 is involved in photomovement, as it is associated with a flagellar gene cluster immediately downstream and

with which it is probably coregulated. A gene for SRII is presumably absent in *Salinibacter*, so it is plausible that PYP could take over its role in mediating a blue-light photoresponse, although the genetic context near the hypersalinity island suggests a role in osmotic regulation.

In conclusion, Sr PYP is the first PYP characterized from a non-photosynthetic organism and is likely to be expressed and functional. The photocycle is similar to that of Hh PYP, including intermediates I_1, I_2, and I_2'. However, it has the slowest recovery of any PYP and is the first occasion where PYP is found as a functional dimer, which is most likely formed through the 31 amino acid N-terminal extension. Sr PYP is stabilized by ionic strength and is the first example of a truly halophilic PYP.

ACKNOWLEDGMENT

The laboratory of Dr. Nancy Horton is thanked for the use of their PC1 photon counting spectrofluorometer.

REFERENCES

1. Sharma, A. K., Spudich, J. L., and Doolittle, W. F. (2006) Microbial rhodopsins: Functional versatility and genetic mobility, *Trends Microbiol. 14*, 463−469.
2. Vierstra, R. D., and Davis, S. J. (2000) Bacteriophytochromes: New tools for understanding phytochrome signal transduction, *Semin. Cell Dev. Biol. 11*, 511−521.
3. Franklin, K. A., Larner, V. S., and Whitelam, G. C. (2005) The signal transducing photoreceptors of plants, *Int. J. Dev. Biol. 49*, 653−664.
4. Gomelsky, M., and Klug, G. (2002) BLUF: A novel FAD-binding domain involved in sensory transduction in microorganisms, *Trends Biochem. Sci. 27*, 497−500.
5. Cusanovich, M. A., and Meyer, T. E. (2003) Photoactive yellow protein: A prototypic PAS domain sensory protein and development of a common signaling mechanism, *Biochemistry 42*, 4759−4770.
6. Kyndt, J. A., Meyer, T. E., and Cusanovich, M. A. (2004) Photoactive yellow protein, bacteriophytochrome, and sensory rhodopsin in purple phototrophic bacteria, *Photochem. Photobiol. Sci. 3*, 519−530.
7. Yooseph, S., Sutton, G., Rusch, D. B., Halpern, A. L., Williamson, S. J., Remington, K., Eisen, J. A., Heidelberg, K. B., Manning, G., Li, W., Jaroszewski, L., Cieplak, P., Miller, C. S., Li, H., Mashiyama, S. T., Joachimiak, M. P., van Belle, C., Chandonia, J. M., Soergel, D. A., Zhai, Y., Natarajan, K., Lee, S., Raphael, B. J., Bafna, V., Friedman, R., Brenner, S. E., Godzik, A., Eisenberg, D., Dixon, J. E., Taylor, S. S., Strausberg, R. L., Frazier, M., and Venter, J. C. (2007) The Sorcerer II Global Ocean Sampling Expedition: Expanding the universe of protein families, *PLoS Biol. 5*, 432−466.
8. Meyer, T. E. (1985) Isolation and characterization of soluble cytochromes, ferredoxins, and other chromophoric proteins from the halophilic phototrophic bacterium *Ectothiorhodospira halophila*, *Biochim. Biophys. Acta 806*, 175−183.
9. Meyer, T. E., Yakali, E., Cusanovich, M. A., and Tollin, G. (1987) Properties of a water-soluble, yellow protein isolated from a halophilic phototrophic bacterium that has photochemical activity analogous to sensory rhodopsin, *Biochemistry 26*, 418−423.
10. Devanathan, S., Brudler, R., Hessling, B., Woo, T. T., Gerwert, K., Getzoff, E. D., Cusanovich, M. A., and Tollin, G. (1999) Dual photoactive species in Glu46Asp and Glu46Ala mutants of photoactive yellow protein: A pH-driven color transition, *Biochemistry 38*, 13766−13772.
11. Ujj, L., Devanathan, S., Meyer, T. E., Cusanovich, M. A., Tollin, G., and Atkinson, G. H. (1998) New photocycle intermediates in the photoactive yellow protein from *Ectothiorhodospira halophila*: Picosecond transient absorption spectroscopy, *Biophys. J. 75*, 406−412.
12. Genick, U. K., Soltis, S. M., Kuhn, P., Canestrelli, I. L., and Getzoff, E. D. (1998) Structure at 0.85 Å resolution of an early protein photocycle intermediate, *Nature 392*, 206−209.
13. Borucki, B., Devanathan, S., Otto, H., Cusanovich, M. A., Tollin, G., and Heyn, M. P. (2002) Kinetics of proton uptake and dye binding by photoactive yellow protein in wild type and in the E46Q and E46A mutants, *Biochemistry 41*, 10026−10037.
14. Jiang, Z., Swem, L. R., Rushing, B. G., Devanathan, S., Tollin, G., and Bauer, C. E. (1999) Bacterial photoreceptor with similarity to photoactive yellow protein and plant phytochromes, *Science 285*, 406−409.
15. Kyndt, J. A., Fitch, J. C., Meyer, T. E., and Cusanovich, M. A. (2007) The photoactivated PYP domain of *Rhodospirillum centenum* Ppr accelerates recovery of the bacteriophytochrome domain after white light illumination, *Biochemistry 46*, 8256−8262.
16. Berleman, J. E., Hasselbring, B. M., and Bauer, C. E. (2004) Hypercyst mutants in *Rhodospirillum centenum* identify regulatory loci involved in cyst cell differentiation, *J. Bacteriol. 186*, 5834−5841.
17. Sprenger, W. W., Hoff, W. D., Armitage, J. P., and Hellingwerf, K. J. (1993) The eubacterium *Ectothiorhodospira halophila* is negatively phototactic, with a wavelength dependence that fits the absorption spectrum of the photoactive yellow protein, *J. Bacteriol. 175*, 3096−3104.
18. Hou, S., Saw, J. H., Lee, K. S., Freitas, T. A., Belisle, C., Kawarabayasi, Y., Donachie, S. P., Pikina, A., Galperin, M. Y., Koonin, E. V., Makarova, K. S., Omelchenko, M. V., Sorokin, A., Wolf, Y. I., Li, Q. X., Keum, Y. S., Campbell, S., Denery, J., Aizawa, S., Shibata, S., Malahoff, A., and Alam, M. (2004) Genome sequence of the deep-sea γ-proteobacterium *Idiomarina loihiensis* reveals amino acid fermentation as a source of carbon and energy, *Proc. Natl. Acad. Sci. U.S.A. 101*, 18036−18041.
19. Mongodin, E. F., Nelson, K. E., Daugherty, S., Deboy, R. T., Wister, J., Khouri, H., Weidman, J., Walsh, D. A., Papke, R. T., Sanchez Perez, G., Sharma, A. K., Nesbo, C. L., MacLeod, D., Bapteste, E., Doolittle, W. F., Charlebois, R. L., Legault, B., and Rodriguez-Valera, F. (2005) The genome of *Salinibacter ruber*: Convergence and gene exchange among hyperhalophilic bacteria and archaea, *Proc. Natl. Acad. Sci. U.S.A. 102*, 18147−18152.
20. Anton, J., Oren, A., Benlloch, S., Rodriguez-Valera, F., Amann, R., and Rossello-Mora, R. (2002) *Salinibacter ruber* gen. nov., sp. nov., a novel, extremely halophilic member of the bacteria from saltern crystallizer ponds, *Int. J. Syst. Evol. Microbiol. 52*, 485−491.
21. Oren, A., Heldal, M., Norland, S., and Galinski, E. A. (2002) Intracellular ion and organic solute concentrations of the extremely halophilic bacterium *Salinibacter ruber*, *Extremophiles 6*, 491−498.
22. Roessler, M., and Muller, V. (2001) Chloride dependence of glycine betaine transport in *Halobacillus halophilus*, *FEBS Lett. 489*, 125−128.
23. Kyndt, J. A., Vanrobaeys, F., Fitch, J. C., Devreese, B. V., Meyer, T. E., Cusanovich, M. A., and Van Beeumen, J. J. (2003) Heterologous production of *Halorhodospira halophila* holophotoactive yellow protein through tandem expression of the postulated biosynthetic genes, *Biochemistry 42*, 965−970.
24. Simondsen, R. P., and Tollin, G. (1983) Transient kinetics of redox reactions of flavodoxin: Effects of chemical modification of the flavin mononucleotide prosthetic group on the dynamics of intermediate complex formation and electron transfer, *Biochemistry 22*, 3008−3016.
25. Yokoyama, H., and Matsui, I. (2005) A novel thermostable membrane protease forming an operon with a stomatin homologue from the hyperthermophilic archaebacterium *Pyrococcus horikoshii*, *J. Biol. Chem. 280*, 6588−6594.
26. Louie, G. V., Bowman, M. E., Moffitt, M. C., Baiga, T. J., Moore, B. S., and Noel, J. P. (2006) Structural determinants and modulation of substrate specificity in phenylalanine-tyrosine ammonia-lyases, *Chem. Biol. 13*, 1327−1338.
27. Gulick, A. M., Lu, X., and Dunaway-Mariano, D. (2004) Crystal structure of 4-chlorobenzoate:CoA ligase/synthetase in the unliganded and aryl substrate-bound states, *Biochemistry 43*, 8670−8679.
28. Genick, U. K., Borgstahl, G. E., Ng, K., Ren, Z., Pradervand, C., Burke, P. M., Srajer, V., Teng, T. Y., Schildkamp, W., McRee, D. E., Moffat, K., and Getzoff, E. D. (1997) Structure of a protein photocycle intermediate by millisecond time-resolved crystallography, *Science 275*, 1471−1475.
29. Oren, A., and Mana, L. (2002) Amino acid composition of bulk protein and salt relationships of selected enzymes of *Salinibacter ruber*, an extremely halophilic bacterium, *Extremophiles 6*, 217−223.

30. Hennig, L., and Schafer, E. (2001) Both subunits of the dimeric plant photoreceptor phytochrome require chromophore for stability of the far-red light-absorbing form, *J. Biol. Chem. 276*, 7913−7918.
31. Sang, Y., Li, Q. H., Rubio, V., Zhang, Y. C., Mao, J., Deng, X. W., and Yang, H. Q. (2005) N-Terminal domain-mediated homodimerization is required for photoreceptor activity of Arabidopsis cryptochrome 1, *Plant Cell 17*, 1569−1584.
32. Anderson, S., Dragnea, V., Masuda, S., Ybe, J., Moffat, K., and Bauer, C. (2005) Structure of a novel photoreceptor, the BLUF domain of AppA from *Rhodobacter sphaeroides*, *Biochemistry 44*, 7998−8005.
33. Laan, W., Gauden, M., Yeremenko, S., van Grondelle, R., Kennis, J. T. M., and Hellingwerf, K. J. (2006) On the mechanism of activation of the BLUF domain of AppA, *Biochemistry 45*, 51−60.
34. Bernard, C., Houben, K., Derix, N. M., Marks, D., van der Horst, M. A., Hellingwerf, K. J., Boelens, R., Kaptein, R., and van Nuland, N. A. (2005) The solution structure of a transient photoreceptor intermediate: Δ25 photoactive yellow protein, *Structure 13*, 953−962.
35. Vreede, J., van der Horst, M. A., Hellingwerf, K. J., Crielaard, W., and van Aalten, D. M. (2003) PAS domains. Common structure and common flexibility, *J. Biol. Chem. 278*, 18434−18439.
36. Frishman, D., and Argos, P. PREDATOR: Protein secondary structure prediction from a single sequence or a set of sequences, http://bioweb.pasteur.fr/seqanal/interfaces/predator-simple.html.
37. Brudler, R., Meyer, T. E., Genick, U. K., Devanathan, S., Woo, T. T., Millar, D. P., Gerwert, K., Cusanovich, M. A., Tollin, G., and Getzoff, E. D. (2000) Coupling of hydrogen bonding to chromophore conformation and function in photoactive yellow protein, *Biochemistry 39*, 13478−13486.
38. Meyer, T. E., Devanathan, S., Woo, T., Getzoff, E. D., Tollin, G., and Cusanovich, M. A. (2003) Site-specific mutations provide new insights into the origin of pH effects and alternative spectral forms in the photoactive yellow protein from *Halorhodospira halophila*, *Biochemistry 42*, 3319−3325.
39. Kyndt, J. A., Hurley, J. K., Devreese, B., Meyer, T. E., Cusanovich, M. A., Tollin, G., and Van Beeumen, J. J. (2004) *Rhodobacter capsulatus* photoactive yellow protein: Genetic context, spectral and kinetics characterization, and mutagenesis, *Biochemistry 43*, 1809−1820.
40. Meyer, T. E., Tollin, G., Causgrove, T. P., Cheng, P., and Blankenship, R. E. (1991) Picosecond decay kinetics and quantum yield of fluorescence of the photoactive yellow protein from the halophilic purple phototrophic bacterium, *Ectothiorhodospira halophila*, *Biophys. J. 59*, 988−991.
41. Kyndt, J. A., Savvides, S. N., Memmi, S., Koh, M., Fitch, J. C., Meyer, T. E., Heyn, M. P., Van Beeumen, J. J., and Cusanovich, M. A. (2007) Structural role of tyrosine 98 in photoactive yellow protein: Effects on fluorescence, gateway, and photocycle recovery, *Biochemistry 46*, 95−105.
42. Getzoff, E. D., Gutwin, K. N., and Genick, U. K. (2003) Anticipatory active-site motions and chromophore distortion prime photoreceptor PYP for light activation, *Nat. Struct. Biol. 10*, 663−668.
43. Hoff, W. D., van Stokkum, I. H., van Ramesdonk, H. J., van Brederode, M. E., Brouwer, A. M., Fitch, J. C., Meyer, T. E., van Grondelle, R., and Hellingwerf, K. J. (1994) Measurement and global analysis of the absorbance changes in the photocycle of the photoactive yellow protein from *Ectothiorhodospira halophila*, *Biophys. J. 67*, 1691−1705.
44. Hoersch, D., Otto, H., Joshi, C. P., Borucki, B., Cusanovich, M. A., and Heyn, M. P. (2007) Role of a conserved salt bridge between the PAS core and the N-terminal domain in the activation of the photoreceptor photoactive yellow protein, *Biophys. J. 93*, 1687−1699.
45. Meyer, T. E., Tollin, G., Hazzard, J. H., and Cusanovich, M. A. (1989) Photoactive yellow protein from the purple phototrophic bacterium, *Ectothiorhodospira halophila*. Quantum yield of photobleaching and effects of temperature, alcohols, glycerol, and sucrose on kinetics of photobleaching and recovery, *Biophys. J. 56*, 559−564.
46. Van Brederode, M. E., Hoff, W. D., Van Stokkum, I. H., Groot, M. L., and Hellingwerf, K. J. (1996) Protein folding thermodynamics applied to the photocycle of the photoactive yellow protein, *Biophys. J. 71*, 365−380.
47. Genick, U. K., Devanathan, S., Meyer, T. E., Canestrelli, I. L., Williams, E., Cusanovich, M. A., Tollin, G., and Getzoff, E. D. (1997) Active site mutants implicate key residues for control of color and light cycle kinetics of photoactive yellow protein, *Biochemistry 36*, 8−14.
48. Devanathan, S., Genick, U. K., Canestrelli, I. L., Meyer, T. E., Cusanovich, M. A., Getzoff, E. D., and Tollin, G. (1998) New insights into the photocycle of *Ectothiorhodospira halophila* photoactive yellow protein: Photorecovery of the long-lived photobleached intermediate in the Met100Ala mutant, *Biochemistry 37*, 11563−11568.
49. Rajagopal, S., and Moffat, K. (2003) Crystal structure of a photoactive yellow protein from a sensor histidine kinase: Conformational variability and signal transduction, *Proc. Natl. Acad. Sci. U.S.A. 100*, 1649−1654.
50. Balashov, S. P., Imasheva, E. S., Boichenko, V. A., Anton, J., Wang, J. M., and Lanyi, J. K. (2005) Xanthorhodopsin: A proton pump with a light-harvesting carotenoid antenna, *Science 309*, 2061−2064.
51. Boichenko, V. A., Wang, J. M., Anton, J., Lanyi, J. K., and Balashov, S. P. (2006) Functions of carotenoids in xanthorhodopsin and archaerhodopsin, from action spectra of photoinhibition of cell respiration, *Biochim. Biophys. Acta 1757*, 1649−1656.
52. Spudich, J. L. (2006) The multitalented microbial sensory rhodopsins, *Trends Microbiol. 14*, 480−487.

BI701486N